UCRL- 95913 Rev. 1
PREPRINT

# DENSITY OF TRAPPED GAS IN HEAVILY IRRADIATED LITHIUM HYDRIDE

R. C. BOWMAN, JR., AND A. ATTALLA
Monsanto Research Corporation - Mound

P. C. SOUERS, C. L. FOLKERS, T. MCCREARY,
G. D. SNIDER, F. VANDERHOOFVEN and
R. T. TSUGAWA

This paper was prepared for submittal to
Journal of Nuclear Materials

July 1987

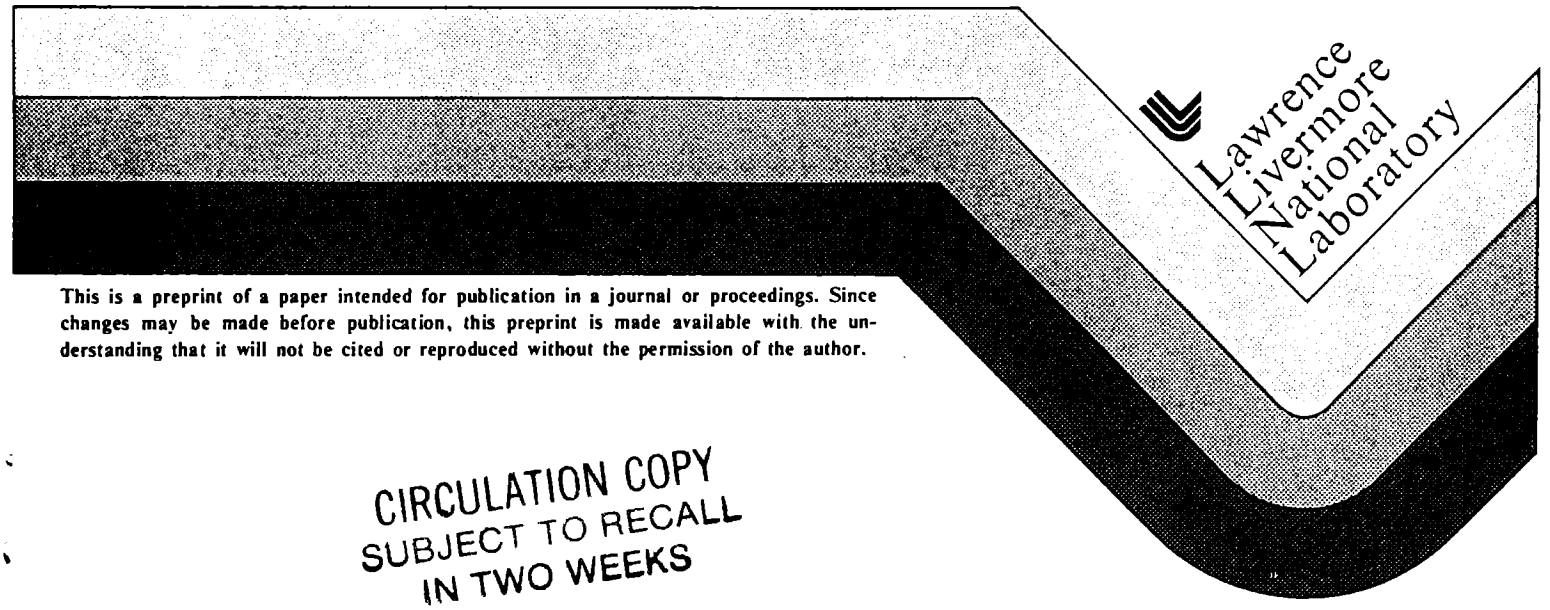

# DENSITY OF TRAPPED GAS IN HEAVILY IRRADIATED LITHIUM HYDRIDE

R. C. BOWMAN, JR.,* and A. ATTALLA
Monsanto Research Corporation - Mound
Miamisburg, OH 45342 U.S.A.

and

P. C. SOUERS, C. L. FOLKERS, T. MCCREARY, G. D. SNIDER,
F. VANDERHOOFVEN and R. T. TSUGAWA
Lawrence Livermore National Laboratory
Livermore, CA 94550 U.S.A.

## ABSTRACT

We review old gamma-irradiated lithium hydride data as well as display much new bulk and gas-displacement density and nuclear magnetic resonance data on Li(D,T) and LiT at 296 to 373 K. We find that 1) Li(D,T) swells because of the formation of internal D-T and $He^3$ gas bubbles, but probably not because of the precipitation of lithium metal. 2) The gas bubbles are at densities of at least 3 to 4 x $10^4$ $mol/m^3$, i.e., thousands of atmospheres. 3) Outgassing may be largely the result of bubbles rupturing, although diffusion of $He^3$ as atoms may occur at long times.

*Now at Aerospace Corporation, El Segundo, CA

The previous paper in this journal summarizes many years of measurement on the radiation-created swelling and outgassing of Li(D,T)[1]. The incorporation of tritium makes it easy to study the hydride behavior to very large doses of radiation. These data, with a suitable algorithm, can probably be used to estimate neutron damage in lithium hydride as well. In this paper, we shall consider the density of internally trapped gas giving rise to the swelling.

## 1. Introduction

Even ionic compounds undergo massive radiation damage at high enough doses. Spaepen observed lithium fluoride to swell as much as 22 volume % after heavy neutron irradiation[2]. Broad-line nuclear magnetic resonance (n.m.r.) by Bray, et. al., showed motionally-narrrowed lines attributed to molecular fluorine and lithium metal[3], thereby demonstrating that the neutron irradiation caused decomposition with the products being trapped.

Pretzel did the first major study of radiation damage on lithium deuteride-tritide, Li(D,T)[4]. He saw large volumetric swelling and noted that it came at the same doses as it did for lithium fluoride. Much of his data is summarized in the preceeding paper. He noted that the "moderate" room temperature swelling increased considerably at 323 to 398 K. He also saw motionally-narrowed hydrogen and lithium n.m.r. signals.

The distinctive shape of the swelling curves are shown illustrated by three examples of Li(D,T) in fig. 1. The initial tritium was 45

mol %, with 55% deuterium. The percent volumetric swelling, as measured by bulk means, is shown, and it is large. At 323 and 348 K, the swelling proceeds in two distinct regions: I - early fast growth and II - slower linear growth. At 298 K, the swelling is slower and does not show the two distinct regions.

Souers, et. al., were the first to study irradiated lithium hydride with pulsed n.m.r., which made quantitative nuclear-counting of the trapped, motionally-narrowed species much easier[5]. The decomposition products showed slowly-decaying n.m.r. signals as constrasted with the rapid, microsecond decays of the ions. The work showed a strong correlation between the tritium n.m.r. signal and the swelling in Li(H,T) samples. After more work by Souers, which we shall review shortly, Bowman and Attalla extended the n.m.r. studies of the trapped hydrogen, helium-3 and lithium in Li(D,T)[6-8]. However, much of this work was not published and will be reported here.

It seems strange, in retrospect, that no one stated in so many words that gas bubbles cause the swelling of irradiated lithium hydride. We believe the evidence presented here makes strong case for this statement.

## 2. Gamma-Irradiated Lithium Hydride

### 2.1. Nuclear Magnetic Resonance

We shall first review the old Souers' work on lithium hydride single crystals irradiated with 1 MeV gamma rays in a 100,000 curie $Co^{60}$ source[9,10]. Although reported, it has not been adequately summarized. We measured the swelling by floating the samples in heated liquid

hydrocarbons. Motionally-narrowed H and $Li^7$ signals were observed by pulsed n.m.r.[11]. The zero-time free induction decay heights were referenced to standard samples of hydrogen and lithium[10]. The trapped hydrogen signal was proved to come from molecular $H_2$ by letting the sample sit at 77 K and watching the rotational odd-J states de-exite to the even-J states[9], where J is the molecular rotational quantum member[12]. The transverse nuclear relaxation time, $T_2$, changed as a single crystal of irradiated lithium hydride was rotated in the magnet[13]. This led to the suggestion that the trapped hydrogen was in cubic bubbles. These bubbles were seen by the scanning electron microscope on carbon replicas of the hydride surface[14]. The bubbles were indeed cubic and with their walls alligned generally in the (100) direction.

Attempts were made to use the relaxation times of the trapped $H_2$[9,10]. The longitudinal relaxation time[15], $T_1$, had been shown to increase with increasing density, $\rho$[16,17]. At room temperature, the Lipsicas-Bloom data fit the relation

$$T_1 \simeq 2.3 \times 10^{-3} \rho + 1.0 \times 10^{-12} \rho^3 \qquad (1)$$

where $T_1$ is in ms and $\rho$ is in $mol/m^3$. The highest densities measured appear to have been about 3000 $mol/m^3$ at room temperature. Equation 1 gave a means of calculating the gas density from $T_1$ as long as the bubble walls were assumed to have no effect on $T_1$. Indeed, $T_1$ did not change when the lithium hydride single crystal was rotated.

It was also noted that the $T_2$, transverse relaxation time, values of the trapped $H_2$ varied considerably. These time constants were calibrated against the measured average bubble edge size, a, as seen by the scanning electron microscope. A transverse wall relaxation time $T_{2w}$ was defined as

$$\frac{1}{T_{2w}} = \frac{1}{T_2} - \frac{1}{T_1} \tag{2}$$

This subtracts out the $T_1$ mechanism as it affects $T_2$. For $T_2 << T_1$, as in the case for most bubbles, then $T_{2w} = T_2$. In the range of $4 < T_{2w} <$ 200 ms (or $8 < a < 70$ nm), the relation was

$$a \simeq 15 \ln T_{2w} - 13 \tag{3}$$

where a is in nm and $T_{2w}$ in ms. The smaller is the bubble, the faster a nuclear magnetic moment crosses to a wall and is dephased in a collision. For very small bubbles, eq. 3 was extrapolated to the hydride ion $T_2$ of about 10 μs in its "bubble" i.e. ionic diameter, of about 0.4 nm[18,19]. For 10 μs $< T_{2w} <$ 4 ms, we have

$$a \sim 4 T_{2w}^{1/2} \tag{4}$$

It was recognized that the $Li^7$ transverse relaxation time $T_2$ also was undoubtedly a function of the metal particle grain size, but no direct calibration was available[20].

## 2.2. Swelling Results

The raw data from the gamma-irradiated lithium hydride experiments have never been shown, and we shall need it. We, therefore, list it in table 1. The dose in MJ/kg is really set for one gram of the starting material. We also convert it to "equivalent days of lithium tritide" irradiation, where fresh LiT absorbs 9.3 MJ/kg·day. This conversion will allows us to compare this data with our new work with tritium. We define the % of swelling by liquid or gas displacement by

$$\alpha = \frac{V_g - V_g(0)}{V_g(0)} (100) \tag{5}$$

Here, $V_g(0)$ is the volume of the unirradiated solid.

The percent of trapped hydrogen seen by n.m.r., $f_H$, is in atomic percent, so as to give a ready measure of the lithium hydride decomposition. The measured number of hydrogen nuclei has been multiplied by 4/3 to give $f_H$, in order to correct for the even-J molecules, which are invisible to n.m.r.

The quantity $f_{Li}$ is the measured atomic % of lithium-7 (in natural lithium), which has a transverse relaxation time long enough to appear in our receiver. We assumed that if $T_2 > 50$ μs for the lithium that it was present as bulk metal. All signals showed the Knight shift characteristic of the metal.

Next we calculate

$$b = \frac{f_{Li}}{f_H} \tag{6}$$

This is the fraction of lithium that has precipitated as metal and given rise to a long-$T_2$ n.m.r. signal. The important point is to note that b never rises to 1, but instead remains at a maximum value of about 0.8. If we consider one mol of LiH with a density of $0.775 \times 10^3$ kg/m$^3$ and a molecular weight of $7.950 \times 10^{-3}$ kg/mol, then the molar volume of the LiH, V(0), is $1.026 \times 10^{-5}$ m$^3$/mol[19,21]. Lithium metal has a molecular weight of $6.942 \times 10^{-3}$ kg/mol and a density of $0.534 \times 10^3$ kg/m$^3$ for a molar volume of $1.300 \times 10^{-5}$ m$^3$/mol. The lithium metal has a larger molar volume than the hydride. The ratio of hydride-to-metal volumes is 0.79, which is close to the maximum value of b that we see. It appears that the lithium metal never causes swelling but only fills hydride space that has been vacated.

It appears, then, that only hydrogen gas causes swelling in the gamma irradiation case. The radiation produces $f_H$ percent of trapped hydrogen, where we define $f_H$ in atomic percent, so that we can easily observe the % decomposition of the hydride. We may divide $f_H$ by 2 to convert to mols of the diatomic gas. The gas density, $\rho$ (in mol/m$^3$), is obtained by dividing the mols of trapped hydrogen by the gas volume. Two possible volumes may be considered.

The easiest way to calculate the density is from

$$\rho = \frac{f_H}{2\alpha V_g(0)} \tag{7}$$

The volume here is the swelling volume, all attributed to hydrogen gas. We are assuming that all the original volume in the hydride is filled equally well by neutral lithium atoms or metallic lithium. The only

difference is whether the lithium has migrated to form larger particles.

Our model assumes that the volume that contained decomposed LiH is not available for hydrogen bubbles. We say, then, that the remaining neutral lithium atoms take up the space originally occupied by lithium and hydride ions. Our model is perhaps the simplest, but certainly it is not the only one.

Table 1 lists the derived gas densities in succeeding columns. The values from eqs. 1 and 7 are in good agreement considering the two very different approaches.

We next take the eq. 7 gas densities and convert them to pressures by means of compressibilities, which we derive in appendix A. We see that the gas pressures are high. The bubbles edge lengths are obtained from eqs. 3 and 4. If we convert the well-known soap bubble problem[22] to a cubic bubble with only one surface, we obtain the equation.

$$\gamma = \frac{Pa}{4} \tag{8}$$

Here, $\gamma$ is the surface tension of the solid and P the bubble pressure. Equation 8 is supposed to hold only if the bubble is in equilibrium with the solid. We may compare the surface tension values in table 1 with the calculated value for lithium fluoride at 0 K[23]. This is 0.5 $J/m^2$ along the (100) plane. Without knowing whether our bubbles are in equilibrium, we would have to say that the agreement is good.

## 3. Nuclear Magnetic Resonance of Lithium Tritide

### 3.1. Equipment and Procedure

We now turn to lithium hydride containing tritium, whose 5.7 keV beta particle is easily capable of ionizing molecules along its path. The tritium half-life is 12.3 years. Although lithium hydride is white, the tritium radioactivity quickly turns it coal black with color centers. We previously studied Li(D,T) with pulsed n.m.r.[5-8], where again, only the long-decay signals characteristic of gas could be seen in the receiver. For samples kept at 296, 343 and 398 K, the tritium n.m.r. signal grew to 4 to 8 at% and tracked with the swelling. This work covered only region I, with the fast swelling.

In this section, we shall present new and more detailed n.m.r. data for 98-99% lithium-7 tritide (containing 1-2% hydride-deuteride). The principles of quantitative nuclear signal counting by pulsed n.m.r. have already been considered[24,25] and preliminary data presented[6-8], and we shall but recapitulate here. The spectrometer was a pulsed Bruker B-KR 323s. The frequency was 23.3 MHz for $Li^7$ and 45.7 MHz for $He^3$ and T. Nuclear counts were taken by applying a $\pi/2$ pulse and observing the free induction decay. The decay, extrapolated back to time zero, is a measure of the absolute number of nuclei causing the signal. Power and receiver recovery time were not crucial, because we were observing motionally-narrowed signals of 50 μs to 1 ms decay time. The spin count standard for $He^3$ and T was protium in $H_2O$ added to 99.99 at% $D_2O$ with $MnCl_2$ present to shorten the longitudinal relaxation time. The standard for $Li^7$ was lithium chloride dissolved in the same

solvent. Nuclear counts, in atomic % of the total initial atoms, have these accuracies: 0.2 ± 0.2%; 2 ± 0.5%; 10 to 15 ± 1%. All n.m.r. measurements were made at room temperature, although the sample, in some cases, was kept at a higher temperature between n.m.r. runs.

Molecular tritium comes in two forms, as determined by the rotational quantum number J. Even-J (para) $T_2$ has no n.m.r. signal but odd-J (ortho) $T_2$ does. The latter form is present at 75 mol% at room temperature, so that the measured n.m.r. nuclear count must be multiplied by 4/3 to include all the tritium.

The longitudinal relaxation times ($T_1$) were measured by nulling out the free induction decay following a $\pi$-$\pi/2$ pulse sequence. The transverse relaxation times ($T_2$) were measured by the Gill-Meiboom $\pi/2$-continuous $\pi$-continuous spin echo sequence. This was different from the Carr-Purcell $\pi/2$-$\pi$-spin echo sequence[26] used in the gamma-irradiated lithium hydride work.

The LiT was synthesized from the elements in iron crucibles. The lithium was melted and the desired amount of tritium added at 1020 K until the reaction ceased. The sample was allowed to slowly cool under 0.3 MPa of gas. The hydride froze at about 960 K, and it took several hours for the sample to cool to room temperature. The purity was about 98%, with the remaining 2% being LiH and LiD with about 0.1% oxygen and 0.01% carbon. The tritide was hand-ground and sieved for all grain sizes under 420 μm (40-mesh). The samples were pressed at room temperature to a bulk value of 90% of theoretical density. The sample dimensions were 5 mm diameter and 15 mm length. The hydride samples were handled in

a dry argon atmosphere and were sealed in evacuated Pyrex tubes. The length of the lithium tritide cylinders was measured, and the swelling was assumed to be isotropic. The fractional increase in length of the hydride samples is $\Delta L/L_o$, where $\Delta L$ is the length change and $L_o$ is the length at zero time. The same quantities for volume are $\Delta V_b$ and $V_b(0)$, where the sub-"b" indicates a bulk measurement. We assume isotropic swelling and use the relation

$$\beta = \frac{V_b - V_b(0)}{V_b(0)} (100) \simeq 300 \left[ \frac{\Delta L}{L_o} + \left( \frac{\Delta L}{L_o} \right)^2 \right] \qquad (9)$$

We ignore the cubed $\Delta L$ term, which is very small.

## 3.2. Results and Discussion

Figure 2 shows the data taken on a composite of three lithium tritide samples kept at 296 K. The free tritium and $He^3$ are both in atomic % of the tritium in the LiT, i.e., we are looking at the % decomposition. We see that the free tritium and $He^3$ together track the swelling. At 800 days, 70% of the $He^3$ remains in the sample. The free lithium precipitates suddenly at 450 days.

Figure 3 shows similiar data for one sample kept at 348 K. The free tritium levels off with 15% trapped inside the solid. The free lithium follows close behind, and the free $He^3$ is also present. It appears that the tritium causes the initial swelling, and the lithium and $He^3$ signals correlate with the later, reduced swelling. Only 40% of the $He^3$ born remains in the sample at 800 days.

Figure 4 shows the triton relaxation times for the trapped tritium in the LiT. We see that $T_1$ is about the same at all temperatures and over all the times. The same is true for the $T_2$ data at 348 and 373 K. The $T_2$ data at 296 K is a decade lower.

Next, we smooth the data of figs. 2 through 4 and present it, with additional 373 K data, in table 2. The time in days allows us a direct comparison with the LiT-equivalent days in table 1. The % bulk swelling is determined from eq. 9. The next three columns contain n.m.r. spin counts for trapped tritium, helium-3 and lithium-7, respectively. The listings of $f_H$, $f_{He}$ and $f_{Li}$ are in atomic % of the LiT, where the measured tritium data has been multiplied by the 4/3 correction factor. The quantity $f_{He}^T$ is the total $He^3$ formed by the tritium decay. It is

$$f_{He}^T = F_T \left[1 - \exp(-t/\tau)\right] \tag{10}$$

where $\tau$ is the tritium decay time constant of 6494 days[27], and $F_T$, the percent of tritium in the hydrogen. For LiT, this is essentially 100%.

The lithium precipitation coefficient of Eq. 6 must be rewritten to account for the tritium decay. We now use the formula:

$$b = \frac{f_{Li}}{f_H + f_{He}^T} \tag{11}$$

Again, this is the fraction of lithium that has precipitated as metal. Neutral lithium forms when tritium goes to form bubbles (or outgas, but we have no measure of this) or when tritium decays to $He^3$. We assume that the lithium is bulk metal when its transverse relaxation time is long enough to show a free induction decay in our receiver, whose dead-time usually masks the ionic signals which have $T_2 < 10$ μs. The characteristic Knight shift of bulk lithium metal is always present in the narrowed signals. At high metal concentrations, it is difficult even to set the π/2-pulse length, due to skin depth effects arising from the formation of very large particles of lithium metal.

In Fig. 5, we plot the lithium precipitation coefficient b as a function of time. Again, it never goes to 1.0. Lithium tritide, with natural lithium, has a molecular weight of $9.958 \times 10^{-3}$ kg/mol and a density of $0.986 \times 10^3$ kg/m$^3$[19,21]. This leads to a ratio of tritide-to-metal molar volume of 0.78, essentially the value we got for lithium hydride.

We next determine the gas density from

$$\rho \simeq \frac{1}{\beta V_b(0)} \left[ \frac{f_H}{2} + f_{He}^T \right] \qquad (12)$$

where we assume that helium-3 as well as tritium causes the swelling. For LiT, $V_b(0)$ is $1.01 \times 10^{-5}$ m$^3$/mol. Equation 12 is not really what we want. We wish we had the gas displacement swelling, α, instead of a bulk value that can contain other voids. We assume also above that all of the $He^3$ causes swelling.

Table 2 lists the calculated densities for gas in LiT. Those obtained from the longitudinal relaxation times are too high. The presence of $He^3$ in the tritium bubbles has apparently destroyed eq. 1 as a pressure sensor. We accept the eq. 12 densities as being the correct ones, because these values are in agreement with the results of table 1.

We next convert the eq. 12 densities to pressures using appendix B and proceed as before to the bubble size and surface tension. These results are listed in table 1. The surface tension numbers are in good agreement with those of table 1 and the calculated literature value[23].

We now turn to the $He^3$ relaxation times, which are shown in fig. 6. The longitudinal relaxation time $T_1$ is constant in the range of about 10 s. This is not especially long for $He^3$, which does not strongly interact with other magnetic moments because of its atomic character. However, $T_1$ is determined in large part by the properties of the wall that it hits[28-31], and we cannot determine the density from it. The transverse relaxation time, $T_2$, should have the same behavior we saw with hydrogen. An increasing $T_2$ should indicate an increasing bubble size. Unfortunately, we have no way to make this quantitative. It appears from fig. 6, however, that the helium bubble size may be increasing with time. This is different from the hydrogen case, where the bubble size stays constant.

## 4. Li(D,T) Swelling and Outgassing

### 4.1. Equipment and Procedure

These are the only Li(D,T) samples for which two different densities, bulk and gas displacement, were simultaneously measured, along with the outgassing. This data was taken in the years 1967 to 1975 and was not correlated with the previously described n.m.r. work of 1973 to 1977. The Li(D,T) was synthesized as previously described. The product was ground and sieved and was pressed into cylindrical compacts at 210 MPa (30 kpsi) and at 378 K or 423 K. Most of the samples were pressed in the first two weeks after synthesis to avoid the difficulties casued by radiation-induced hardness (see appendix B). The initial bulk densities were 86 $\pm$ 3% of the theoretical crystal density. The lithium was 95.6 mol% of the 6-isotope in all cases. We do not expect this to be factor, becuase the molar volume of $Li^6$ is only 0.13% larger than that of $Li^7$[32].

The hydride samples were always handled in an argon atmosphere, with 1 to 2 ppm water vapor, 5 ppm $O_2$, and 20 to 500 ppm $N_2$. Nitriding of lithium metal occurred only occasionally. Fresh hydride made in this box contained 0.015 at% oxygen, as measured by Karl Fischer analysis. After 71 days, the oxygen increased to 0.03 to 0.07 at%. Unfortunately, because of the measuring technique, the samples were exposed to the box atmosphere for each density taken.

The Li(D,T) swelling was measured two ways. The first was the bulk measurement, i.e., the dimensional one. the samples were removed from their heated cans and allowed to cool to room temperature. Then, the

lengths of the 20 mm by 19 mm cylindrical hydride samples were hand-measured with a micrometer to ± 0.005 mm, with five readings being taken on each sample. The mass was measured to ±0.5 mg. Equation 9 for isotropic growth was used in converting length to volume.

On five samples, the diameters were also measured. These were #169 to #173 with 20%-initial tritium and kept at 298, 323 and 348 K. The length-to-diameter ratio increased only 0.2 to 0.3% in the first 100 days and remained constant thereafter to the end at 1700 to 3300 days. The assumption of isotropic growth, based on these samples, appears to be valid. Using this assumption, we believe $V_b(0)$ to be accurate to the nearest 0.1%.

The second method of measuring Li(D,T) swelling was by gas displacement, using a Beckman 930 air comparison pycnometer. This was made up of two piston-cylinders, each brought to the same pressure. One cylinder had the sample in it, and the volume it occupied was read off a scale. Steel balls were used as volume standards. The mass of the sample was needed to derive the density. The accuracy in measuring the percent swelling was again to the nearest ±0.1%. Unfortunately, powder, as well as the pressed cylinder, was kept in each can, so that the gas came from both.

Before opening the cans for the density measurements, the gas was removed, and the total amount measured by pressure-volume-temperature. Accuracies were: for less than 50 μmol, ±20% of the measured value; 50 to 500 μmol, ±5%; greater than 500 μmol, ±1%. The samples were then analyzed on a high-resolution, magnetic-sector mass spectrometer for the mol%

of hydrogen isotopes and $He^3$. If the gas sample was less than 50 μmol, then the errors in determining the mol% were ±3% for hydrogen and ±10% for $He^3$. For samples larger than 250 μmol, the errors are ±1% and ±5 mol%, respectively.

An example of all the measurements made simultaneously on one sample is shown in fig. 7 for #172 with 20% initial tritium kept at 323 K. The two distinctive swelling regions I and II are evident in the bulk density curve.

## 4.2. Outgassing from Ruptured Bubbles

In fig. 7, we note the progressively widening difference between the bulk and gas displacement swellings, α and β. We shall consider the proposition that this volume originally contained gas bubbles which have ruptured, so that the volume is now accessible to the entrance of measuring gas.

We wish to compare swelling and outgassing. We use the two densities we have available to calculate the % volume difference, ΔV, defined by

$$\Delta V = 100\left\{[V_b(t) - V_b(0)] - [V_g(t) - V_g(0)]\right\} / V(0) \qquad (13)$$

$$= \frac{\beta V_b(0) - \alpha V_g(0)}{V(0)}$$

This is the percent of space that gas can reach in the expanded sample. The gas that has come off the sample, in units of atomic %, is $(f_H^o/2 + f_{He}^o)$. In fig. 8, we plot, for the five 323 K samples, ΔV along the x-axis and the % outgassing along the y-axis. We find a correlation

between the quantities that suggests that bubble rupture is the cause of the outgassing.

We shall expand this observation into a model, where we assume that all outgassing comes from ruptured bubbles. Gas displacement measures swelling caused by gas still trapped in the solid. The density of the gas will be

$$\rho = \frac{(f_H/2) + f_{He}}{\alpha V_g(0)} \tag{14}$$

Bulk measurements see all swelling that has occured whether the gas is still inside or not. In this case, the gas density is

$$\rho = \frac{(f_H + f_H^o)/2 + f_{He}^T}{\beta V_b(0)} \tag{15}$$

where $f_H^o$ is the at% of hydrogen that has outgassed from the sample.

If we eliminate $f_H/2$, we calculate the gas density

$$\rho = \frac{f_H^o/2 + (f_{He}^T - f_{He})}{\beta V_b(0) - \alpha V_g(0)} \tag{16}$$

The amount of internally trapped hydrogen will be

$$f_H = 2\left[\rho\alpha V_g(0) - (f_{He}^T - f_{He}^o)\right] \tag{17}$$

In the equation above, $f_{He}$ has been replaced by $f^{T}_{He} - f^{o}_{He}$, where $f^{o}_{He}$ is the at% of outgassed helium.

We now apply these calculations to the two-density Li(D,T) samples, and the results are summarized in table 3. There is considerable scatter, probably partly from the errors in subtraction plus unknown history of the samples. The calculated gas density starts low, at about $10^3$ mol/m$^3$ and reaches $10^4$ mol/m$^3$ at the times shown. We next average the densities and trapped hydrogen concentrations from the the $10^4$ mol/m$^3$ date to the end of the experiment. We find seven sets of samples where the density is under $3 \times 10^4$ mol/m$^3$. For these, we find

$$\rho \simeq (2.4 \pm 1.0) \times 10^4 \text{ mol/m}^3 \tag{18}$$

$$f_H \simeq 8 \pm 5 \text{ at\%} \tag{19}$$

Four sets have densities over $4 \times 10^4$ mol/m$^3$. Here,

$$\rho \simeq (4.2 \pm 2.0) \times 10^4 \text{ mol/m}^3 \tag{20}$$

$$f_H \simeq 19 \pm 13 \text{ at\%} \tag{21}$$

The reason for the apparent division of the data in this way is unknown. Of course, if the density is high, so will be the trapped hydrogen concentration. A constant or rising density was the most common feature. Four sets showed greatly increased densities at the end. For example, the last two points for #279 were at 1600 and 2600 days. Here,

the densities were 7 x $10^4$ mol/$m^3$ and the hydrogen concentrations were 50 at%. The latter number is difficult to believe, and it is triggered in our equations by a sudden pouring of $He^3$ out of the sample. In these cases, we may wonder if this $He^3$ was really inside a bubble. At long times and for higher tritium concentrations, it may be that the helium diffuses to the surface as atoms.

The low densities at early times is questionable. If crack space without gas existed to the extent of 10% of the bulk swelling, the bubble density would be over 2 x $10^4$ mol/$m^3$ even at early times.

In conclusion, however, this data appears to generally confirm our earlier supposition: that gas bubbles exist at densities of tens of mol/$m^3$ containing roughly 10 at% of the internal hydrogen as well as much or all of the $He^3$.

## 5. Conclusions

We may summarize this work with the following observations for Li(D,T) at 296 to 373 K.

1. Li(D,T) swells because of internally trapped D-T and $He^3$ gas. At 323 to 373 K, the D-T causes rapid early swelling and then shuts off. The $He^3$ causes a slow linear swelling thereafter.

2. The gas bubbles are at densities of at least 3 to 4 x $10^4$ mol/$m^3$, which translates into hundreds of MPa (thousands of atmospheres).

3. Much of the outgassing appears to be caused by rupturing bubbles. Atomic diffusion of helium could also add to the outgassing.

4. Lithium metal appears not to cause swelling, even though its molar volume is larger than that of lithium hydride.

At 323 and 348 K, we can now guess which gases are responsible for regions I and II. As seen in the data[1], the early outgassing is almost all hydrogen. This, coupled with the n.m.r. data, suggests that the trapped hydrogen is the dominant cause of region I. The $He^3$, which is created more slowly, is the probable cause of region II.

But there is an interesting scientific question in regard to this. Why does the formation of trapped D-T gas bubbles shut off? This phenomenon causes the sudden decrease in slope in the bulk swelling at these two temperatures. Table 4 shows the trapped tritium in five samples at 348 K and 378 K in region II. The tritium is constant in four samples and drops slightly in one. There are two possible answers as to why the internal decomposition shuts off.

1. That lithium precipitation is the key to shutting off the decomposition by increasing back reaction. It could do this by penetrating into the swelling space,raising the D-T gas pressure and finally reacting with the D-T back hydride. The n.m.r. spin count data is insufficient to settle this question, although no abrupt increase in $T_1$ is seen. For this mechanism to be true, we would have to switch to another model than the one used in this paper.

2. That the total amount of trapped hydrogen is the key to establishing an equilibrium between the hydride and the elements. Some sort of model containing the number of bubbles and their sizes plus the location of the lithium, would have be made. The unusual feature of

lithium hydride is that it traps so much gas inside rather than just letting it go free.

Acknowledgments

Work performed under the auspices of the U.S. Department of Energy by M.R.C.-Mound Laboratqry under Contract No. DE-AC04-76-DP00053 and the Lawrence Livermore National Laboratory under contract No. W-7405-ENG-48.

## Appendix A. Compressibility of Hydrogen Gas

In order to convert gas densities to pressures for the D-T bubbles, we use $H_2$ and $D_2$ compressibilities from the literature[33-34]. We shall write the compressibility z as

$$z = 1 + AP + BP^2 \qquad (22)$$

where A and B are pressure coefficients listed in table 5. The pressure, P, is in MPa. Equation 22 may be used from 50 to 600 MPa, where we have extrapolated past the data. The highest measured compressibilities are 230 to 290 MPa at 296 to 423 K and 180 MPa at 473 to 538 K. Although the data is derived for $H_2$ and $D_2$ we used it for D-T and $T_2$ without worrying about the small isotopic differences.

## Appendix B. Pressing of Li(D,T) Compacts

The bulk density of Li(D,T) compacts is a function of the pressure used to form them, as shown in fig. 9 up to 280 MPa (40 kpsi). The Y-axis is the ratio of the initial bulk density to the theoretical crystal density. For best results, the hydride should be fresh, which means two weeks old or less in fig. 9. The best results are obtained at 423 K. More scattered results occur at pressing temperatures of 378 to 398 K.

Aging the hydride hardens it and makes it more difficult to press. We measured the hardness using the Vickers diamond-point indentation method[35]. The hardness H is defined as

$$H = \frac{P}{0.539d^2} \tag{23}$$

where P is the load in kg and d is the diagonal of indentation, in mm. We are interested in the relative change in hardness. Immediately after synthesis, the hardness is about 40 kg/(mm)$^2$ for Li(D,T). The 3.8 MJ/mol sample in fig. 9 hardened to 163 kg/(mm)$^2$ after being stored for 182 days at room temperature. The 45 MJ/mol sample measured at 134 kg/(mm)$^2$ after 400 days at 243 K. However, another 500 days at room temperature passed before the curve of fig. 9 was taken.

Figure 10 shows the hardness of Li(D,T) samples with 10 to 40% initial tritium over the first days after synthesis. The hardness

increases with the initial percent of tritium. The hardness also increases with time, so that a sample should be pressed as soon after birth as possible if maximum density is desired.

References

[1] P. C. Souers, F. J. Ackerman, T. J. Biel, J. Bigwood, V. Brite, L. D. Christensen, C. L. Folkers, V. Gede, C. M. Griffith, E. B. Huss, R. Lindahl, T. McCreary, H. H. Otsuki, R. L. Pond, G. D. Snider, C. Stanhope, R. K. Stump, F. Vanderhoofven, R. T. Tsugawa, J. L. Anderson, D. H. W. Carstens, W. L. Drumhiller, W. B. Lewis, J. E. Nasise, F. E. Pretzel, E. G. Szklarz, D. T. Vier, R. C. Bowman, Jr. and A. Attalla, "Swelling and Outgassing of Heavily Irradiated Lithium Hydride," J. Nucl. Mater., this volume, previous paper.

[2] J. Spaepen, Phys. Rev. Letters 1 (1958) 281 .

[3] C. Knutson, H. Hooper and P. Bray, J. Phys. Chem. Solids 27 (1966) 147.

[4] F. E. Pretzel, D. T. Vier, E. G. Szklarz, and W. B. Lewis, Radiation Effects on Lithium Hydride, Report LA-2463, Los Alamos National Laboratory, Los Alamos, N.M. (1961).

[5] P. C. Souers, T. A. Jolly and C. F. Cline, J. Phys. Chem. Solids 28 (1967) 1717.

[6] R. C. Bowman, Jr. and A. Attalla, "Radiation Damage in LiT," Report MLM-2161 (OP), Monsanto Research Corporation, Mound Laboratory, Miamisburg, OH 45342 (1974) and in Tritium Technology in Fission, Fusion and Isotopic Applications, L. J. Wittenberg, ed. (American Nuclear Society, 1980), p. 108.

[7] R. C. Bowman, Jr., Nature 271 (1978) 531.

[8] R. C. Bowman, Jr. and A. Attalla, Trans. Amer. Nucl. Soc. 28 (1978) 200.

[9] P. C. Souers, T. S. Blake, R. M. Penpraze and C. Cline, J. Phys. Chem. Solids 30 (1969) 2649.

[10] P. C. Souers, T. Imai, T. S. Blake, R. M. Penpraze and H. R. Leider, J. Phys. Chem. Solids 31 (1970) 1461.

[11] In n.m.r., the sample is placed in a dc magnetic field and radiation is applied at the n.m.r. frequency of the particular nucleus. The application of a $\pi/2$-pulse at the n.m.r. frequency causes the nuclei to "fluoresce" in phase. The emitted radiation, also at the n.m.r. frequency, dies out with a time constant set by the magnetic field inhomogeneity or by the sample itself. If the latter case is present, the decay constant is $T_2$, the transverse (sometimes called the spin-spin) relaxation time, i.e. the time constant for the loss of phase coherence. The decay signal from the nuclei is called a free induction decay and its height at time zero (i.e. just as the $\pi/2$-pulse ends) is a direct measure of the number of nuclei creating the signal. Thus can pulsed n.m.r. be used for quantitative analysis.

[12] The diatomic hydrogen molecules have quantized moecular rotational energy levels, listed by the quantum numbers J=0, 1, .... For the heteronuclear hydrogens like HD, excitation between rotational states is instantaneous. For the homonuclear hydrogens, i.e. $H_2$, $D_2$ and $T_2$, it is not. A quantum symmetry rule prevents

even-J-to-odd-J conversion, and slow catalysis is needed to create the transition. This phenomenon is the signature of molecular hydrogen. In old terminology, the even-J states are often called para-$H_2$, ortho-$D_2$ and para-$T_2$. The odd-J states are called ortho-$H_2$, para-$D_2$ and ortho-$T_2$.

[13] P. C. Souers, T. S. Blake and R. M. Penpraze, Phil. Mag. 21 (1970) 287.

[14] T. Imai, Phil. Mag. 21 (1970) 281.

[15] The longitudinal relaxation time, $T_1$, is the time constant for loss of energy in the nuclear magnetic system. It is often called the spin-lattice time, which is often a misnomer because some other mechanism besides the lattice may dominate $T_1$.

[16] M. Lipsicas and M. Bloom, Can. J. Phys. 39 (1961) 881.

[17] M. Bloom, Proc. Int. Conf. Low Temp. Phys. 7th (LT-7, 1961), 61.

[18] Y. S. Oei, H. Richtering and H. D. Wiemhöfer, Ber. Bunsenges Phys. Chem. 83 (1979) 463.

[19] T. N. Mel'nikova, High. Temp.-High. Pressure (Soviet) 13 (1981) 675.

[20] P. C. Souers, T. S. Blake, R. M. Penpraze and H. R. Leider, Further Studies on Irradiated Lithium Hydride: Metal Formation and Thermal Annealing Behavior, Lawrence Livermore National Laboratory Report UCRL-50726 (1969).

[21] J. L. Anderson, J. Nasise, K. Philipson and F. E. Pretzel, J. Phys. Chem. Solids 31 (1970) 613.

[22] W. J. Moore, Physical Chemistry, 3rd ed. (Prentice-Hall, Englewood Cliffs, N.J., 1962), p. 729.

[23] K. S. Yun and G. C. Benson, J. Chem. Phys. 43 (1965) 3980.

[24] A. Attalla and R. C. Bowman, Jr., Anal. Chem. 47 (1975) 728.

[25] A. Attalla and R. C. Bowman, Jr., Anal. Chem., Symp. Ser. 19 (1984) 363.

[26] E. Fukushima and S. B. W. Roeder, Experimental Pulse NMR, A Nuts and Bolts Approach (Addison-Wesley, Reading, MA, 1981), pp. 25-34, 168-172.

[27] C. R. Rudy and K. C. Jordan, "Tritium Half-Life", Report MLM-2458, Monsanto Research Corporation, Mound Laboratory, Miamisburg, OH 45342 (1977).

[28] R. Chapman and M. G. Richards, Phys. Rev. Lett 33 (1974) 18.

[29] W. A. Fitzsimmons, L. L. Tankersley, and G. K. Walters, Phys. Rev. 179 (1969) 156.

[30] R. S. Timsit, J. M. Daniels, and A. D. May, Can. J. Phys. 49 (1971) 560.

[31] J. G. Ganiere, Helv. Phys. Acta 46 (1973) 147.

[32] E. J. Covington and D. J. Montgomery, J. Chem. Phys. 27 (1957) 1030.

[33] A. Michels, W. DeGraaff, T. Wassenaar, J. M. H. Levelt and P. Louwerse, Physica 25 (1959) 25.

[34] D.C. Presnall, J. Geophys. Res. 74 (1969) 6026.

[35] Metals Handbook, H. E. Boyer, ed., 8th ed. (American Society for Metals, Metals Park, Ohio 44073, 1976), XI, 13-14.

Figure Captions

Fig. 1 Examples of bulk swelling in Li(D,T). The samples are #77, 79 and 99 with initial tritium concentrations of 45%. There are two distinct regions at 323 and 348 K: I - early fast growth and II - slow linear growth.

Fig. 2 Linear swelling and n.m.r. results on lithium tritide kept at 296 K.

Fig. 3 Linear swelling and n.m.r. results for lithium tritide kept at 348 K but measured at room temperature.

Fig. 4 Triton n.m.r. relaxation times at 45.7 MHz for trapped tritium in lithium tritide. Gas densities and bubble sizes, at a given temperature, appear constant over the measured time.

Fig. 5 Lithium precipitation coefficient b as determined by nuclear magnetic resonance in lithium at three storage temperatures. The expected maximum at 0.78 is for lithium metal occupying available internal space only. That the coefficient b never exceeds the maximum means that metallic lithium does not cause swelling.

Fig. 6 $He^3$ n.m.r. relaxation times at 45.7 MHz for trapped helium in lithium tritide.

Fig. 7 Data on Li(D,T) sample #172 with 20% initial tritium and kept at 323 K. The swellings are in percent, where $\alpha$ is from gas displacement and $\beta$ from bulk measurements. The outgassing is in mmol gas per original mol of hydride. The helium outgassing is higher than the listed numbers by a factor of three.

Fig. 8 Volume difference between bulk and gas displacement density measurements and outgassing of D-T and $He^3$ from Li(D,T) samples with 10 to 30% initial tritium kept at 323 K. This figure strengthens the argument that outgassing comes from rupturing bubbles.

Fig. 9 Pressing curves for Li(D,T) with 10 to 65 mol % initial tritium. "Fresh" material is less than 2 weeks old. The 3.8 MJ/mol sample had 25% tritium and was kept 182 days at room temperature. The 45 MJ/mol sample had 65% tritium and was kept 905 days at 243 to 298 K.

Fig. 10 The hardness of Li(D,T) increases linearly with time in the first days after synthesis. Storage is at room temperature. This data suggests that compacts should be pressed as soon after synthesis as possible if high densities are desired.

Table 1.
Raw data and calculations for gamma irradiated lithium hydride. All measurements were made at room temperature following the irradiation.

| Temp. (K) | Dose (MJ/kg) | Dose LiT-Equiv. days | % Vol. Swelling, α | Atomic % Trapped $H_2$, $f_H$ | Atomic % Trapped Li, $f_{Li}$ | Li pptn b | Density, ρ ($X10^4$ mol/$m^3$) Eq. 7 | Density, ρ ($X10^4$ mol/$m^3$) Eq. 1 | nmr Relaxation Times $T_1$ (ms) | nmr Relaxation Times $T_2$ (ms) | Pressure, P (MPa) | Bubble Edge Length, a (nm) | Surface Tension, γ ($J/m^2$) |
|---|---|---|---|---|---|---|---|---|---|---|---|---|---|
| 363 | 5 | 0.5 | 0.8 | 0.36 | <0.2 | ~0 | 2.3 | - | - | - | - | - | - |
| | 13 | 1.4 | 1.9 | 1.9 | 0.2 | 0.1 | 5.0 | 5.6 | 310 | 1.9 | 450 | 6 | 0.7 |
| | 70 | 7.5 | 8.2 | 6.6 | 2.0 | 0.30 | 4.0 | 4.6 | 200 | 9.7 | 300 | 22 | 1.6 |
| | 140 | 15 | 11.5 | 9.1 | 6.7 | 0.74 | 4.0 | 4.0 | 160 | 13 | 300 | 27 | 2.0 |
| | 470 | 51 | 17.0 | 5.9 | 2.0 | 0.34 | 1.7 | 3.8 | 140 | 14 | 70 | 29 | 0.5 |
| 398 | 2 | 0.2 | 0.24 | 0.21 | <0.2 | ~0 | 4.4 | - | - | <15 | - | 4 | - |
| | 5 | 0.5 | 1.2 | 1.1 | <0.2 | ~0 | 4.6 | 6.2 | 375 | 1.5 | 500 | 5 | 0.6 |
| | 13 | 1.4 | 5.2 | 5.3 | 1.8 | 0.34 | 5.1 | 5.3 | 270 | 3.7 | 550 | 8 | 1.1 |
| | 35 | 3.8 | 7.4 | 7.1 | 2.6 | 0.37 | 4.8 | 4.8 | 220 | 5.0 | 450 | 9 | 1.0 |
| | 70 | 7.5 | 9.7 | 7.7 | 4.3 | 0.56 | 4.0 | 4.2 | 170 | 10.5 | 300 | 23 | 1.7 |
| | 140 | 15 | 17.0 | 10.4 | 7.4 | 0.71 | 3.1 | 4.1 | 160 | 15 | 200 | 29 | 1.4 |
| | 470 | 51 | 20.5 | 9.6 | 7.9 | 0.82 | 2.3 | 3.5 | 120 | 23 | 120 | 37 | 1.1 |
| 423 | 2 | 0.2 | 0.28 | 0.25 | <0.2 | ~0 | 4.5 | 6.6 | 440 | ~1 | 430 | 4 | 0.4 |
| | 5 | 0.5 | 1.5 | 1.4 | <0.2 | ~0 | 4.7 | 5.7 | 315 | 2.3 | 450 | 6 | 0.7 |
| | 13 | 1.4 | 5.6 | 6.1 | 3.1 | 0.51 | 5.4 | 4.9 | 230 | 6.7 | 600 | 10 | 1.5 |
| | 35 | 3.8 | 8.9 | 7.7 | 4.0 | 0.52 | 4.3 | 4.2 | 175 | 9.8 | 400 | 22 | 2.2 |
| | 70 | 7.5 | 11.5 | 8.1 | 5.5 | 0.68 | 3.5 | 3.8 | 140 | 16 | 260 | 30 | 2.0 |
| | 140 | 15 | 20 | 10.5 | 6.8 | 0.65 | 2.6 | 3.6 | 125 | 22 | 150 | 36 | 1.4 |
| | 470 | 51 | 22 | 11.9 | 9.5 | 0.80 | 2.7 | 2.8 | 88 | 33 | 160 | 47 | 1.9 |
| 473 | 2 | 0.2 | 0.34 | 0.26 | <0.2 | ~0 | 3.8 | 5.3 | 275 | 2.6 | 330 | 7 | 0.6 |
| | 5 | 0.5 | 1.9 | 1.5 | 0.9 | 0.60 | 3.9 | 4.3 | 175 | 6.6 | 350 | 10 | 0.9 |
| | 13 | 1.4 | 7.2 | 5.9 | 4.3 | 0.73 | 4.1 | 3.7 | 135 | 26 | 390 | 39 | 3.8 |
| | 35 | 3.8 | 11.5 | 7.9 | 5.4 | 0.68 | 4.0 | 3.1 | 100 | 35 | 370 | 47 | 4.4 |
| | 70 | 7.5 | 15.2 | 7.2 | 4.8 | 0.67 | 2.4 | 2.7 | 80 | 43 | 160 | 55 | 2.2 |
| | 140 | 15 | 21.2 | 9.1 | - | - | 2.1 | 2.7 | 80 | 45 | 120 | 57 | 1.7 |
| | 280 | 30 | 25.0 | 9.7 | 6.7 | 0.69 | 1.9 | 2.1 | 57 | - | 100 | - | - |
| 538 | 35 | 3.8 | 11.0 | 3.1 | 2.7 | 0.87 | 1.4 | 1.6 | 40 | 30 | 80 | 86 | 1.7 |
| | 280 | 30 | 11.0 | 3.1 | 2.2 | 0.71 | 1.4 | 1.6 | 36 | 33 | 80 | 77 | 1.5 |

Table 2.
Smoothed swelling and n.m.r. nuclear count data on lithium tritide compacts.
All measurements were made at room temperature.

| Time (days) | % Bulk Swelling, β | Trapped gas from nmr nuclear counts (at%) $f_H$ | $f_{He}$ | $f_{Li}$ | Total He, $f^T_{He}$ (%) | Li ppm b | Density, ρ (x10$^4$ mol/m$^3$) Eq. 12 | Eq. 1 | nmr relaxation Times $T_1$ (ms) | $T_2$ (ms) | Pressure, P (MPa) | Bubble Edge Length, a (nm) | Surface Tension, γ (J/m$^2$) |
|---|---|---|---|---|---|---|---|---|---|---|---|---|---|
| 296 K | | | | | | | | | | | | | |
| 50 | 4.0 | 1.5 | 0.0 | 0 | 0.8 | 0 | 3.9 | - | - | - | 240 | - | - |
| 100 | 8.0 | 2.6 | 0.0 | 0 | 1.5 | 0 | 3.5 | - | - | - | 190 | - | - |
| 200 | 14.0 | 4.8 | 2.7 | 0 | 3.0 | 0 | 3.9 | 10 | 300 | - | 240 | - | - |
| 300 | 20.0 | 6.3 | 4.0 | 0 | 4.5 | 0 | 3.8 | 10 | 310 | 1.7 | 230 | 5 | 0.3 |
| 400 | 24.0 | 7.4 | 4.8 | 0 | 6.0 | 0 | 4.0 | 10 | 330 | 1.9 | 240 | 6 | 0.4 |
| 500 | 27.0 | 8.3 | 5.4 | 0.5 | 7.4 | 0.03 | 4.3 | 11 | 380 | 2.1 | 290 | 6 | 0.4 |
| 600 | 29.0 | 8.9 | 5.8 | 6.0 | 8.8 | 0.34 | 4.6 | 12 | 420 | 2.4 | 330 | 6 | 0.7 |
| 700 | 30.5 | 9.3 | 6.2 | 11.5 | 10.2 | 0.59 | 4.9 | 12 | 420 | 2.8 | 390 | 7 | 0.9 |
| 800 | 32.0 | 9.7 | 6.4 | 15.0 | 11.6 | 0.70 | 5.1 | 11 | 390 | 3.2 | 420 | 7 | 0.9 |
| 348 K | | | | | | | | | | | | | |
| 50 | 23.0 | 11.0 | 1.0 | 4.0 | 0.8 | 0.34 | 2.7 | 8 | 240 | - | 140 | - | - |
| 100 | 28.0 | 12.7 | 1.0 | 8.0 | 1.5 | 0.56 | 2.8 | 8 | 250 | - | 140 | - | - |
| 200 | 32.5 | 14.0 | 1.2 | 10.5 | 3.0 | 0.62 | 3.1 | 9 | 260 | - | 160 | - | - |
| 300 | 36.0 | 14.6 | 1.5 | 12.2 | 4.5 | 0.64 | 3.3 | 9 | 270 | 23 | 180 | 20 | 0.9 |
| 400 | 39.0 | 14.9 | 2.0 | 13.6 | 6.0 | 0.65 | 3.4 | 9 | 290 | 20 | 190 | 19 | 0.9 |
| 500 | 41.0 | 15.0 | 2.6 | 15.0 | 7.4 | 0.67 | 3.6 | 10 | 310 | 18 | 210 | 17 | 0.9 |
| 600 | 43.5 | 15.0 | 3.2 | 16.2 | 8.8 | 0.68 | 3.7 | 10 | 320 | 17 | 230 | 17 | 1.0 |
| 373 K | | | | | | | | | | | | | |
| 50 | 23.0 | 13.0 | - | 6.2 | 0.8 | 0.45 | 3.1 | 5 | 280 | 36 | 190 | 26 | 1.2 |
| 100 | 29.1 | 13.6 | - | 9.2 | 1.5 | 0.61 | 2.8 | 5 | 270 | 36 | 150 | 26 | 1.0 |
| 200 | 36.2 | 14.4 | 2.3 | 11.3 | 3.0 | 0.65 | 2.8 | 5 | 260 | 36 | 150 | 26 | 1.0 |
| 300 | - | 14.8 | 2.9 | 12.1 | 4.5 | 0.63 | - | 5 | 270 | 36 | - | 26 | - |
| 400 | - | 15.1 | 3.6 | 13.9 | 6.0 | 0.66 | - | 5 | 280 | 24 | - | 20 | - |
| 600 | - | 15.7 | 3.1 | 15.0 | 8.8 | 0.61 | - | - | - | - | - | - | - |
| 1000 | - | 17.4 | 2.2 | 20.6 | 14.3 | 0.65 | - | 6 | 310 | 33 | - | 24 | - |

Table 3.
Summary of the two-density measurements on various Li(D,T) samples.

| Temp. (K) | Initial % T, $F_{T_i}$ | Sample # | Days to $10^4$ mol/m$^3$ | Maximum days | Averages from $10^4$ mol/m$^3$ to end: Density, $\rho$ ($\times 10^4$ mol/m$^3$) | Averages from $10^4$ mol/m$^3$ to end: Trapped Hydrogen, $f_H$ (at%) | Remarks |
|---|---|---|---|---|---|---|---|
| 298 | 10 | 232 | 400 | 2700 | 2.7 | 6 | peak at 5 x $10^4$ at 900 days |
| | 20 | 169 | 400 | 3300 | 2.7 | 7 | rising; 2 high end points |
| | 30 | 277 | 100 | 2600 | 4.1 | 15 | constant; 2 high end points |
| | 30 | 287 | 250 | 2400 | 2.0 | - | constant; 1 high end point |
| 323 | 10 | 234-5 | 140 | 2700 | 2.3 | 8 | constant from 240 days |
| | 20 | 170-1 | 80 | 3300 | 2.5 | 10 | rising steadily |
| | 20 | 172 | 90 | 3300 | 1.9 | 6 | rising steadily |
| | 30 | 279-80 | 450 | 2600 | 4.0 | 23 | rising; 2 high end points |
| | 30 | 288 | 600 | 2400 | 2.5 | 11 | rising steadily |
| 348 | 10 | 236-7 | 70 | 2700 | 4.6 | 17 | peak of 8 x $10^4$ at 350 days |
| | 20 | 173 | 50 | 1700 | 4.2 | 20 | rising steadily |
| | 30 | 281-2 | 40 | 1200 | 2.2 | 7 | constant after 60 days |

Table 4. Percent of trapped tritium inside lithium tritide stored at 348 K and 373 K. The internal tritium is generally constant in region II.

| Storage Temp(K) | Sample No. | Days Measured | % Trapped tritium, $f_H$ Average | Standard Deviation |
|---|---|---|---|---|
| 348 | DD291A | 11 - 124 | 11.4 | 0.7 |
| | | 173 - 782 | 14.4 | 0.7 |
| | | 951 | 5.7? | - |
| | B84Y | 41 - 328 | 13.2 | 1.1 |
| | | 334 - 951 | 10.9 | 0.5 |
| | B84Z | 41 - 951 | 14.3 | 1.5 |
| 373 | DD299-3 | 51 -1032 | 14.9 | 1.2 |
| | DD326D | 59 - 969 | 14.4 | 0.8 |

Table 5.
Pressure coefficients for the calculation of hydrogen gas compressibilities. The pressures are in MPa and the compressibility is dimensionless. The numbers in parentheses are powers of ten.

| Temp (K) | A[(MPa)$^{-1}$] | B[(MPa)$^{-2}$] |
|---|---|---|
| 296-298 | 6.7246(-3) | -2.5680(-6) |
| 348 | 5.8032(-3) | -2.3616(-6) |
| 363 | 5.5360(-3) | -2.2313(-6) |
| 373 | 5.4161(-3) | -2.2364(-6) |
| 398 | 5.0558(-3) | -2.0168(-6) |
| 423 | 4.7520(-3) | -1.8862(-6) |
| 473 | 4.2239(-3) | -1.7877(-6) |
| 538 | 3.6185(-3) | -1.7504(-6) |

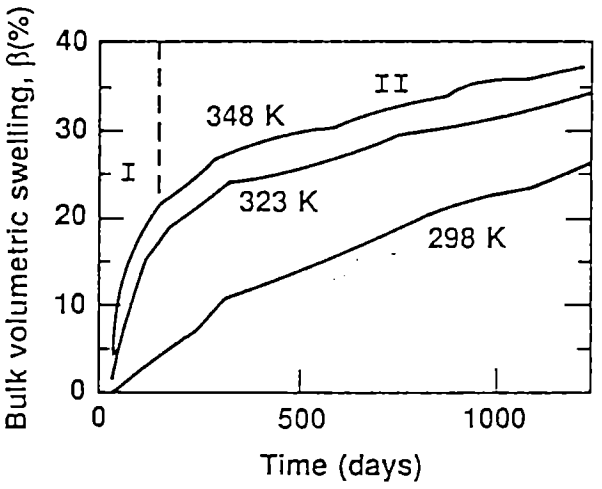
Bulk volumetric swelling, β(%)
40
30
20
10
0
0
500
1000
Time (days)
I
II
348 K
323 K
298 K

F1

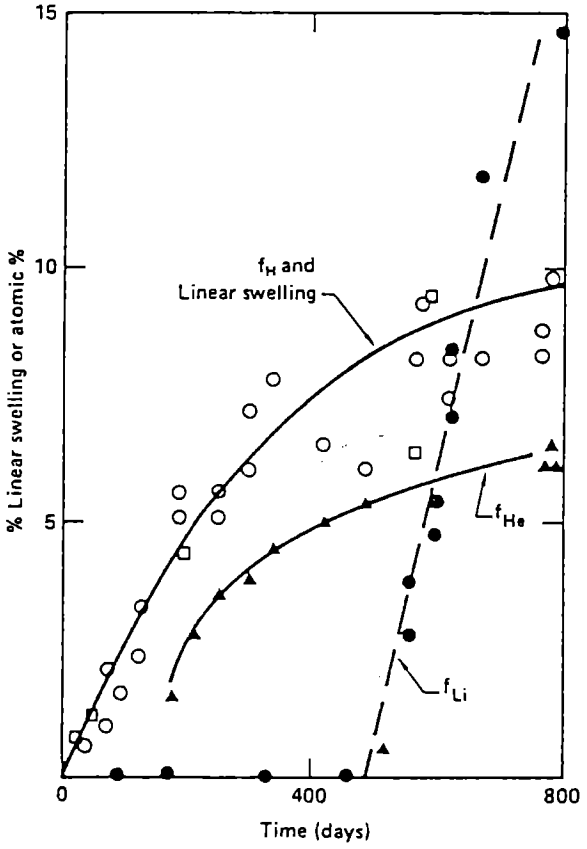
15
10
5
0
400
800
% Linear swelling or atomic %
Time (days)
$f_H$ and
Linear swelling
$f_{He}$
$f_{Li}$

F2

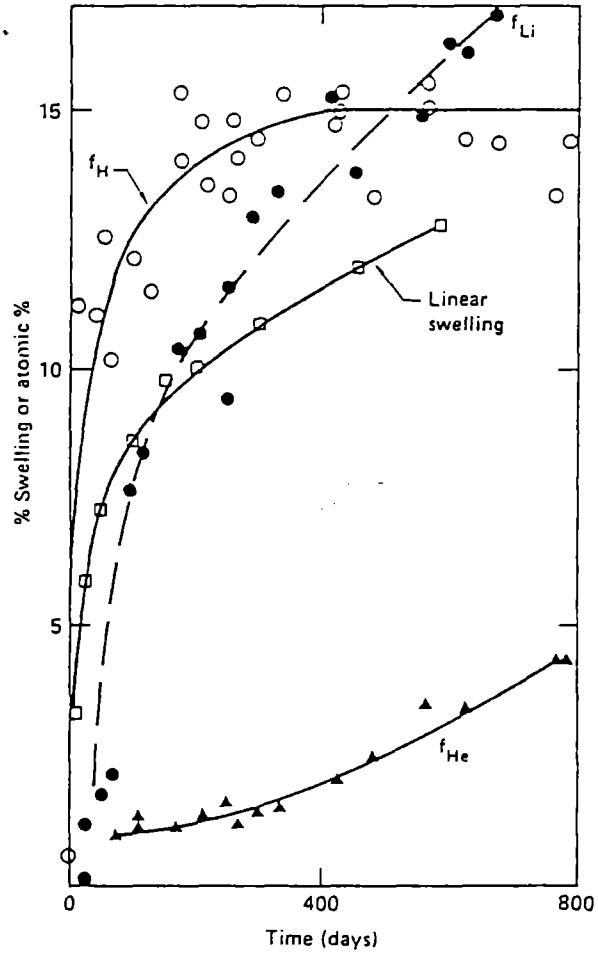
15
10
5
0
400
800
% Swelling or atomic %
Time (days)
$f_{Li}$
$f_H$
Linear swelling
$f_{He}$

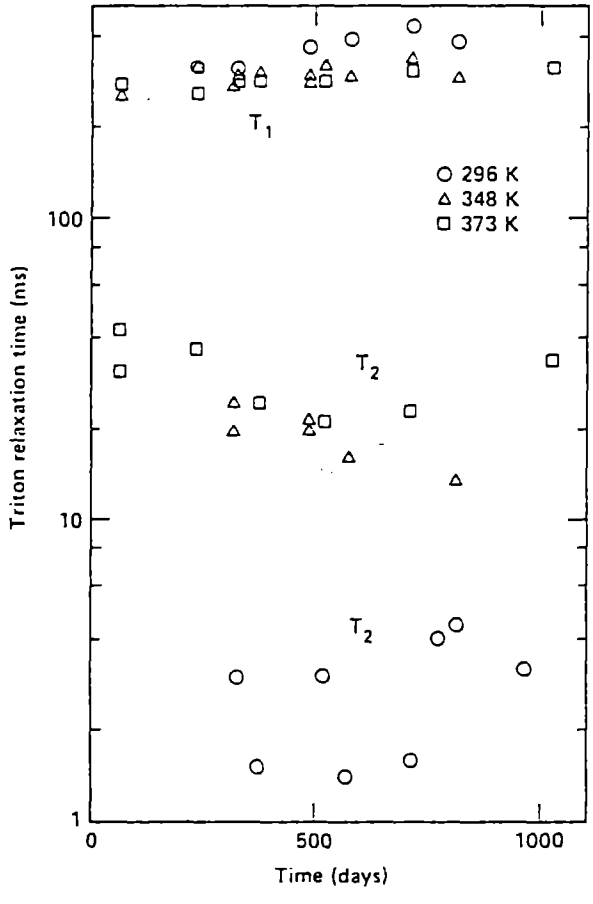
Triton relaxation time (ms)
100
10
1
0
500
1000
Time (days)
T1
T2
T2
296 K
348 K
373 K

F4

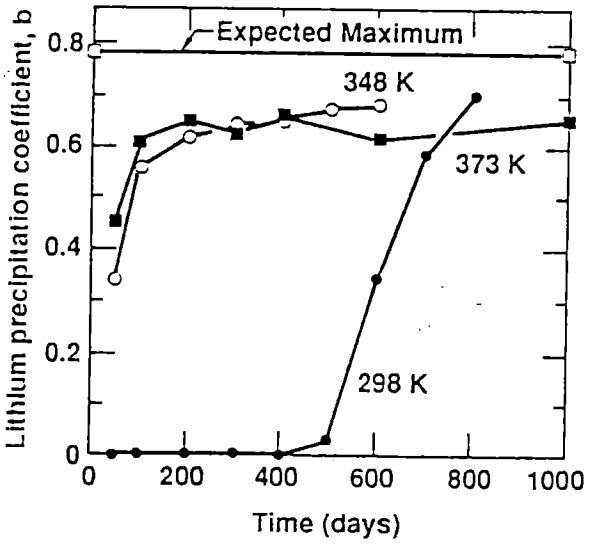
Expected Maximum
348 K
373 K
298 K
Lithium precipitation coefficient, b
0.8
0.6
0.4
0.2
0
0
200
400
600
800
1000
Time (days)

FS

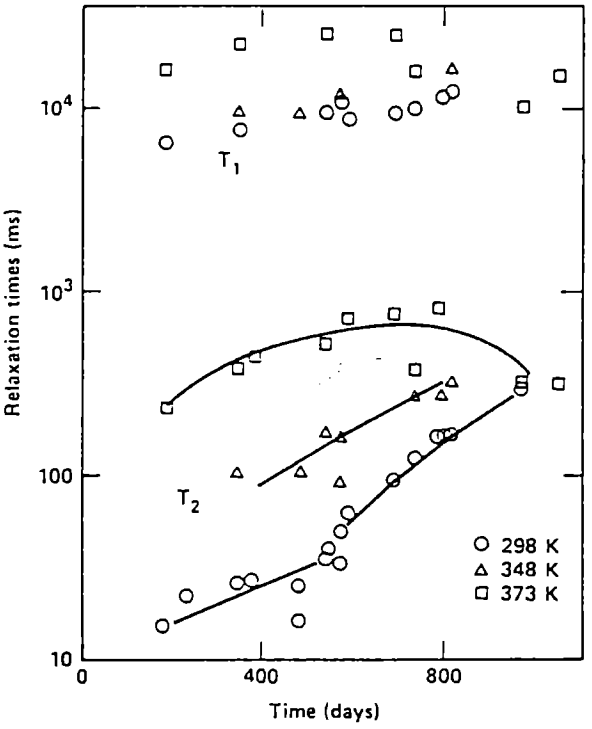
Relaxation times (ms)
$10^4$
$10^3$
100
10
$T_1$
$T_2$
0
400
800
Time (days)
298 K
348 K
373 K

F6

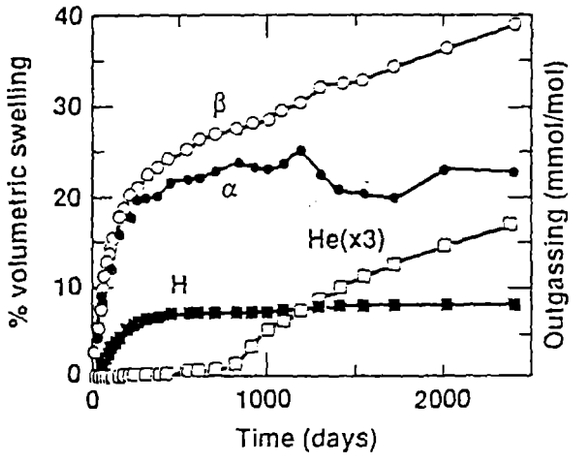
40
30
20
10
0
% volumetric swelling
β
α
He(x3)
H
0
1000
2000
Time (days)
Outgassing (mmol/mol)

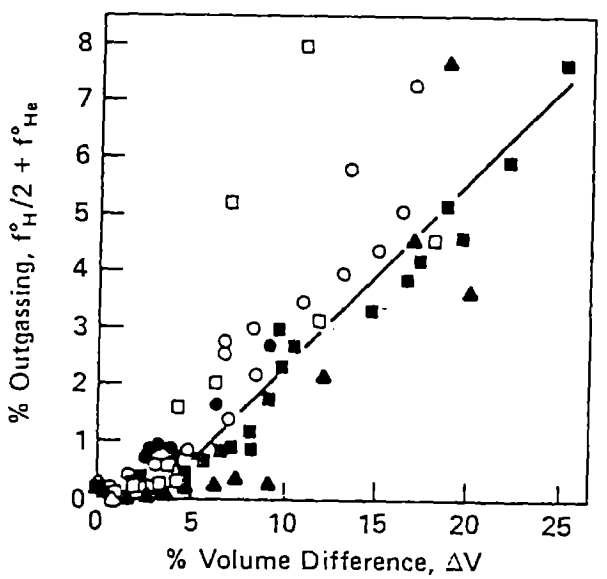
% Outgassing, $f^{\circ}_{H}/2 + f^{\circ}_{He}$
% Volume Difference, ΔV
0
1
2
3
4
5
6
7
8
0
5
10
15
20
25

F8

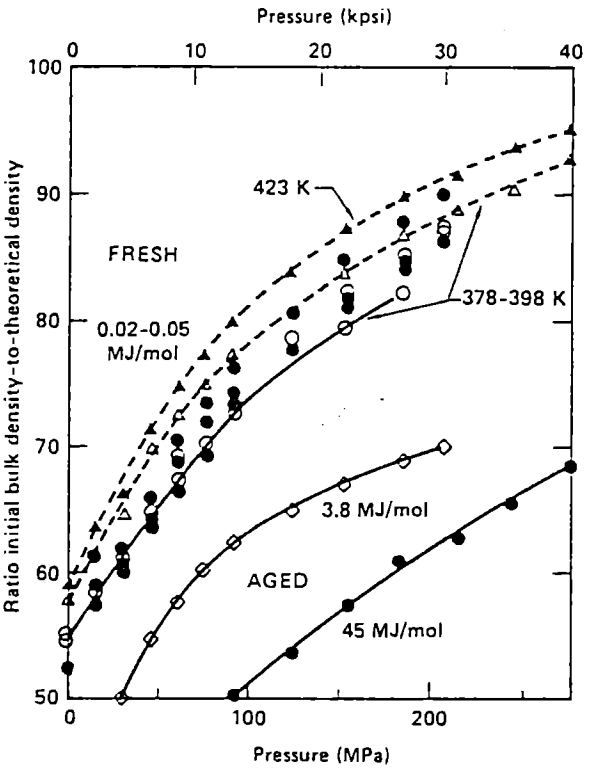
Pressure (kpsi)
0
10
20
30
40
100
90
80
70
60
50
Ratio initial bulk density-to-theoretical density
423 K
FRESH
0.02-0.05
MJ/mol
378-398 K
3.8 MJ/mol
AGED
45 MJ/mol
0
100
200
Pressure (MPa)

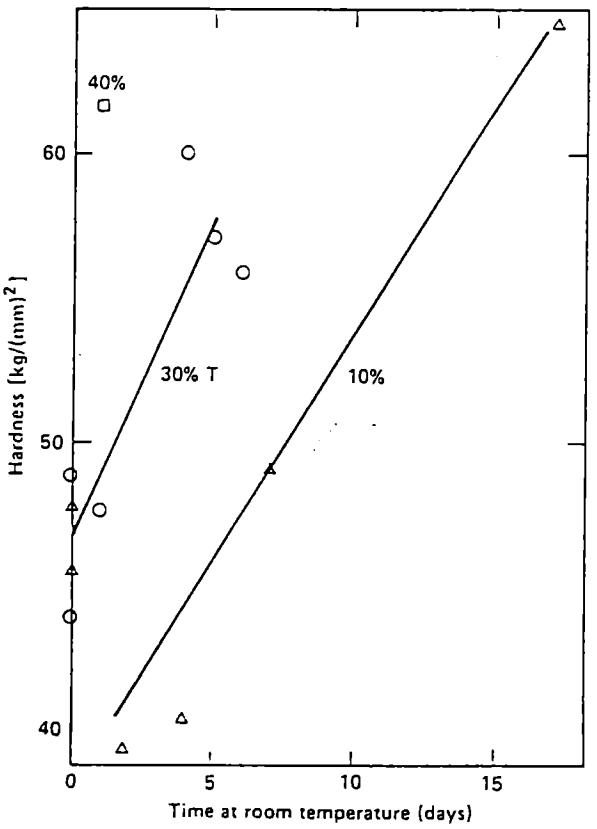
40%
60
50
40
30% T
10%
Hardness [kg/(mm)$^2$]
0
5
10
15
Time at room temperature (days)

F10